A current-source-converter-based PMSG wind energy conversion system: simulation study

Elgenedy, M. A. ; Abdel-Khalik, A. S.; Elserougi, A. A.; Ahmed, S.; Massoud, A.

Published in:
2012 15th International Middle East Power System Conference (MEPCON)

Publication date:
2012

Document Version
Author accepted manuscript

Citation for published version (Harvard):
Elgenedy, MA, Abdel-Khalik, AS, Elserougi, AA, Ahmed, S & Massoud, A 2012, A current-source-converter-based PMSG wind energy conversion system: simulation study. in *2012 15th International Middle East Power System Conference (MEPCON).* IEEE.

A current-source-converter-based PMSG wind energy conversion system: simulation study

Elgenedy, M. A. ; Abdel-Khalik, A. S.; Elserougi, A. A.; Ahmed, S.; Massoud, A.

Published in:
2012 15th International Middle East Power System Conference (MEPCON)

Publication date:
2012

Document Version
Early version, also known as pre-print

Citation for published version (Harvard):
Elgenedy, MA, Abdel-Khalik, AS, Elserougi, AA, Ahmed, S & Massoud, A 2012, A current-source-converter-based PMSG wind energy conversion system: simulation study. in *2012 15th International Middle East Power System Conference (MEPCON).* IEEE, Fifteenth International Middle East Power Systems Conference, Alexandria, Egypt, 23/12/12.

A Current-Source-Converter-Based PMSG Wind Energy Conversion System: Simulation Study

M. A. Elgenedy, A. S. Abdel-Khalik , A. A. Elserougi — *Alexandria University, Egypt*

S. Ahmed — *Texas A&M university at Qatar*

A. Massoud — *Qatar university*

***Abstract*— Wind energy is a prominent area of application of variable-speed generators operating on the constant grid frequency. This paper describes the operation and control of one of these variable-speed wind generators, namely, the Current Source Converter (CSC) based Permanent Magnet Synchronous Generator (PMSG). This generator is connected to the power network by means of a fully controlled frequency converter, which consists of a Pulse Width Modulation (PWM) rectifier, an intermediate dc circuit, and a PWM inverter. The generator is controlled to obtain maximum power from the incident wind by applying flux oriented control (FOC) to the generator side converter (Current Source Rectifier, CSR). On the other hand, voltage oriented control (VOC) is applied the grid-side converter (Current Source Inverter, CSI) to allow unity power factor operation of the windmill and to control the dc-link current. The controller keeps the dc-link current at a minimum value with various wind speeds to reduce the converter power loss at lower power levels. A simulation study is carried out using Matlab/Simulink to simulate the system under different conditions**

***Keywords*— Current source converter (CSC), permanent-magnet synchronous generator (PMSG), Maximum Power Point Tracking (MPPT), space vector modulation (SVM), flux oriented control (FOC), voltage oriented control (VOC).**

Nomenclature

A. Symbols

A	Turbine blades' swept area.
C_i, C_r	Grid- and generator-side converter ac capacitances.
C_p	Turbine-rotor-power coefficient.
i_s, i_g	Grid and generator currents.
i_{ci}, i_{cr}	Grid- and generator-side capacitor currents.
I_{dc}	Generator stator current.
i_{wi}, i_{wr}	Grid- and generator-side converter ac currents.
L_d, L_q	Generator dq-axis synchronous inductances.
L_{dc}	DC-link inductance.
L_o	Grid-side equivalent line inductance.
m_i, m_r	Grid- and generator-side converter modulation indexes.
P	Number of generator pole pairs.
P_m	Generator mechanical power input.
P_g	Generator MPPT real power output.
P_{dc}	DC link inductor power.
P_o, Q_o	Grid-side real and reactive power outputs.
R	Radius of the turbine.
T_e	Generator electromagnetic Torque.
V_{Ldc}	Voltage across the dc-link inductance.
V_s, V_g	Grid and generator voltages.
v_w	Wind speed in meters per second.
α_i , α_r	CSI and CSR polar angles.
β	Pitch angle
θ_g	Grid phase locked loop (PLL) angle.
θ_r	Rotor angle.
θ_{wi}, θ_{wr}	CSI and CSR SVM angles.
λ_r	Generator rotor magnetic flux.
λ	Tip-speed ratio.
ρ	Air density (kilograms per cubic meter).
ω_r	Generator electrical angular frequency.
ω_s	Grid electrical angular frequency.
ω_m	Mechanical rotor speed.

B. Subscripts

d, q	d- and q-axis components.

I. Introduction

The future trend of wind energy conversion systems is to increase the power capacity of wind turbines and generators to reduce the cost of generated electricity [1].

Numerous research efforts have been done for large systems, targeting 5–10 MW level for offshore applications. In these wind energy conversion systems, a direct driven synchronous generator with a full-capacity power converter has been proved to be an effective solution, especially for offshore applications, because of its low maintenance cost, complete decoupling from the grid, wide operating range, and capability of fault ride through. Using permanent magnet on the rotor instead of conventional wound rotor with dc excitation becomes an attractive alternative due to it higher efficiency and the required rotor slip-rings are dispensed [2].

In today's wind energy industry, low-voltage two-level voltage-source converters (VSCs) are dominant for doubly fed induction generator [3], or synchronous generator [4], based wind energy conversion systems. As the power ratings of wind turbines keeps increasing, more low-voltage power converters have to be connected in parallel or in series to handle high power, resulting in a complicated system, low efficiency, and high manufacturing cost. Recently, several high-power converter topologies, such as three-level neutral point clamped (NPC) converter and multilevel modular converter, were proposed for wind energy conversion. These topologies are based on voltage-source inverter technology, and LC filters or complicated zig-zag transformers are often required [5].

In this paper a Current Source Converter (CSC) based Wind Energy Conversion System (WECS) using Permanent Magnet Synchronous Generator (PMSG) is simulated using MATLAB/SIMULINK toolbox. The controller is designed to ensure Maximum Power Point Tracking (MPPT), Zero Direct axis Current control (ZDC) for the generator, DC Link current control that allows power transfer from the generator to the grid, and unity power factor control for grid interface.

The following sections will give a detailed explanation of the system control strategy followed by simulation results to a 2.5MW wind turbine.

II. Maximum Power Tracking

The amount of power captured by the wind turbine (power delivered by the rotor) is given by

$$P_m = 0.5\rho A C_p(\lambda,\beta)\times(v_w)^3 = 0.5\rho A C_p(\lambda,\beta)\times(\frac{\omega_r R}{\lambda})^3 \quad (1)$$

The coefficient C_p of a wind turbine is influenced by the bitch angle and tip speed ratio, which is given by

$$\lambda = \frac{\omega_m R}{v_m} \quad (2)$$

The wind turbine can produce maximum power when the turbine operates at maximum C_p (i.e., at C_{p_opt}). Therefore, it is necessary to keep the rotor speed at an optimum value of the tip-speed ratio λ_{opt} at certain pitch angle. If the wind speed varies, the rotor speed should be adjusted to follow the change [6]-[8]. The target optimum power from a wind turbine can be written as

$$P_{m\_opt} = 0.5\rho A C_{p\_opt}(\frac{\omega_{m\_opt} R}{\lambda_{opt}})^3 = K_{opt}(\omega_{m\_opt})^3 \quad (3)$$

where,

$$K_{opt} = 0.5\rho A C_{p\_opt}(\frac{R}{\lambda_{opt}})^3 \quad (4)$$

$$\omega_{m\_opt} = \frac{\lambda_{opt}}{R} v_w = K_w v_w \quad (5)$$

Therefore, the target optimum torque can be given by

$$T_{m\_opt} = K_{opt}(\omega_{m\_opt})^2 \quad (6)$$

The mechanical rotor power generated by the turbine as a function of the rotor speed for different wind speed is shown in Fig. 1. The optimum power curve (P_{opt}) in Fig.1 shows how maximum energy can be captured from the fluctuating wind.

Fig.1 shows that there is a certain rotor speed produces optimum power for any wind speed. If the controller follows the optimum curve, the wind turbine will produce maximum power at any speed within the allowable range. The generator should operate at optimum torque point, given by (6), which is determined by the MPPT algorithm.

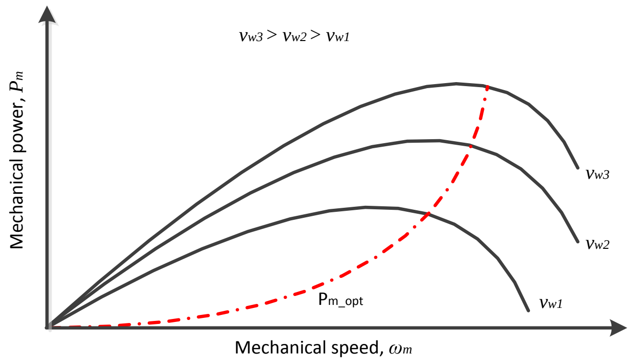

Fig. 1. Mechanical power generated by the turbine as a function of the rotor speed for different wind speeds.

III. System Overview

Fig. 2 shows the structure of a CSC based PMSG variable-speed wind turbine with its controllers. It includes a wind turbine, PMSG, a vector-controlled PWM current-source rectifier, DC-link inductance, and a vector-controlled PWM current-source inverter. The output of MPPT provides references for wind turbine pitch control as well as generator speed control. This paper mainly focuses on the generator and converter control, and therefore, the wind turbine pitch control is not discussed. In this paper, field-oriented control (FOC) is employed at the generator side to guarantee operating at maximum power point with minimum stator current, while voltage-oriented control (VOC) is employed for the grid side to guarantee injecting the desired active power to the grid at unity power factor.

Space vector modulation (SVM) for CSC [9, 10] is used to generate gating signals in both converters. Generally, the current-source converters feature a simple converter structure, low switching *dv/dt*, and reliable overcurrent/short-circuit protection. for both CSCs, IGBT with series connected diode is used as a switching element, where the IGBT transistor has lower losses and can operate at higher switching frequencies [11], and the diode has higher blocking voltage capabilities.

The detailed control scheme of each side will be discussed in the following sections.

IV. Generator Side Control

Fig. 3 shows the generator-side control scheme. The control scheme is developed based on rotor flux oriented synchronous frame [12]. Two control functions are implemented on the generator side: one is to extract maximum power available from the wind turbine and the other is to reduce the generator stator current. Refereed to Fig.3 (grid side), the reference electromagnetic torque is the output of the MPPT algorithm. The quadrature component reference of the grid current (i_{qg}*) can be estimated from the generated reference torque. Generally, the torque of the PMSG can be described as

$$T_e = \frac{3P}{2}[\lambda_r i_{qg} - (L_d - L_q) i_{dg} i_{qg}] \quad (7)$$

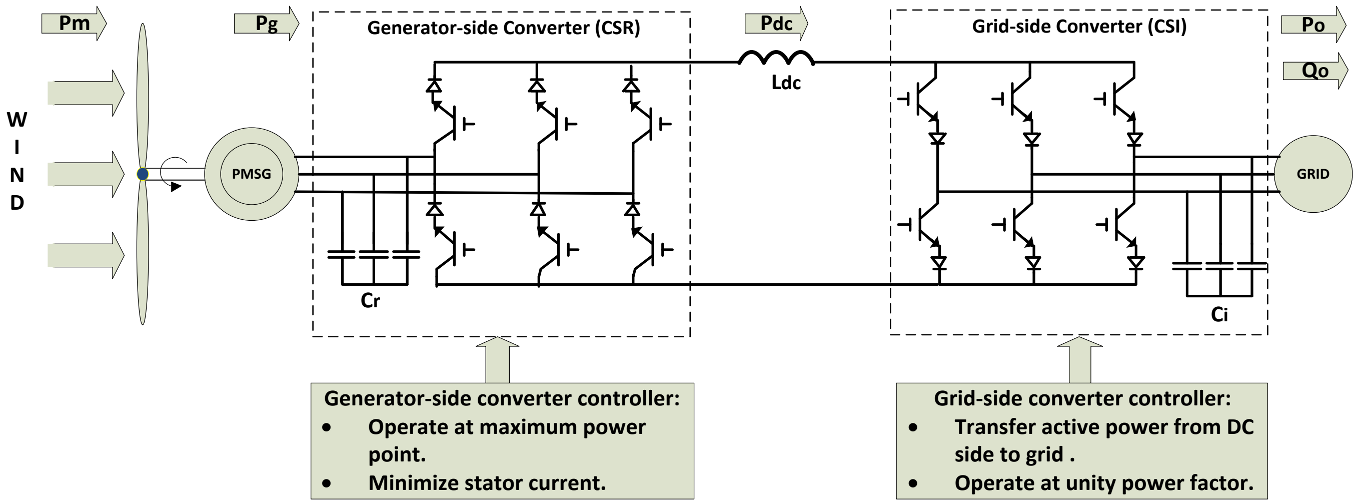

Fig. 2. Structure of a CSC based PMSG variable-speed wind energy conversion system.

In this paper a surface mounted PMSG is used, in this type the d-axis inductance is the same as the q-axis inductance ($L_d = L_q$) thus the reference torque equation is reduced to

$$T_e^* = \frac{3P}{2}[\lambda_r i_{qg}^*] \tag{8}$$

Since (λ_r) is constant, the relation between T^*_e and i^*_{qg} is linear. Thus controlling the q-axis current means controlling the electromagnetic torque and hence, controlling the transferred active power to the generator side converter.

On the other hand, there are several methods to control the d-axis current such as maximum torque per ampere method (MTPA), zero direct current method (ZDC) and unity power factor method (UPF) [8], ZDC method is the same as the MTPA method in case of surface mounted PMSG, and both methods aim to reduce the stator current to achieve minimal stator losses, in this paper ZDC is applied, the direct current is controlled via PI controller to be zero in order to minimize stator losses as in Fig. 3.

From Fig.3, the CSR input current is given by,

$$i_{wr} = i_g - i_{cr} \tag{9}$$

Neglecting the stator resistance and using d-q notation, and taking into account the relation between the capacitor voltage (which is equal to the generator terminal voltage) and the capacitor current yields,

$$i_{dwr} + ji_{qwr} = (i_{dg} + ji_{qg}) - j\omega_r C_r (v_{dg} + jv_{qg}) \tag{10}$$

Hence the *d*- and *q*-axis components of the CSR is given by,

$$i_{dwr} = i_{dg} + \omega_r C_r v_{qg} \tag{11}$$

$$i_{qwr} = i_{qg} - \omega_r C_r v_{dg} \tag{12}$$

From (11) and (12), the modulation index and the SVM phase can be calculated in the stator reference frame for proper operation of the CSR switches where,

$$i_{wr} = \sqrt{(i_{dwr}^2 + i_{qwr}^2)} \tag{13}$$

$$\alpha_r = \tan^{-1}(\frac{i_{qwr}}{i_{dwr}}) \tag{14}$$

Then CSR modulation index and the SVM phase are given by,

$$m_r = \frac{i_{wr}}{I_{dc}} \tag{15}$$

$$\theta_{wr} = \alpha_r + \theta_r \tag{16}$$

V. Grid Side Control

The main control objectives of the grid-side converter are to regulate the dc link current and to achieve zero injected reactive power to the grid. The dc current of the CSC based wind energy system can be controlled by either the rectifier or the inverter, but the latter provides much better dynamic performance and is therefore recommended for practical implementation [13].

If a stiff grid is assumed, the controller is developed based on grid-voltage orientation control, where the synchronous frame is aligned to the grid-voltage space phasor. The control scheme is shown in Fig. 3. Grid-voltage phase-locked loop (PLL) is employed to obtain the synchronous phase θ_s and grid frequency ω_s.

The controller is composed of two independent control loops for real and reactive powers. The dc-current regulator adjusts the real power flow to maintain a certain amount of dc current. Direct reactive power regulation is implemented for a unity power factor reactive power requirement.

With the aligned synchronous frame, the grid voltage has only d-axis component V_{ds} while q-axis component V_{qs} equals to zero. The active and reactive power outputs to the grid can therefore be independently controlled by regulating current outputs to the grid as follows,

$$P_o = 1.5V_{ds} i_{ds} \tag{17}$$

$$Q_o = 1.5V_{ds} i_{qs} \tag{18}$$

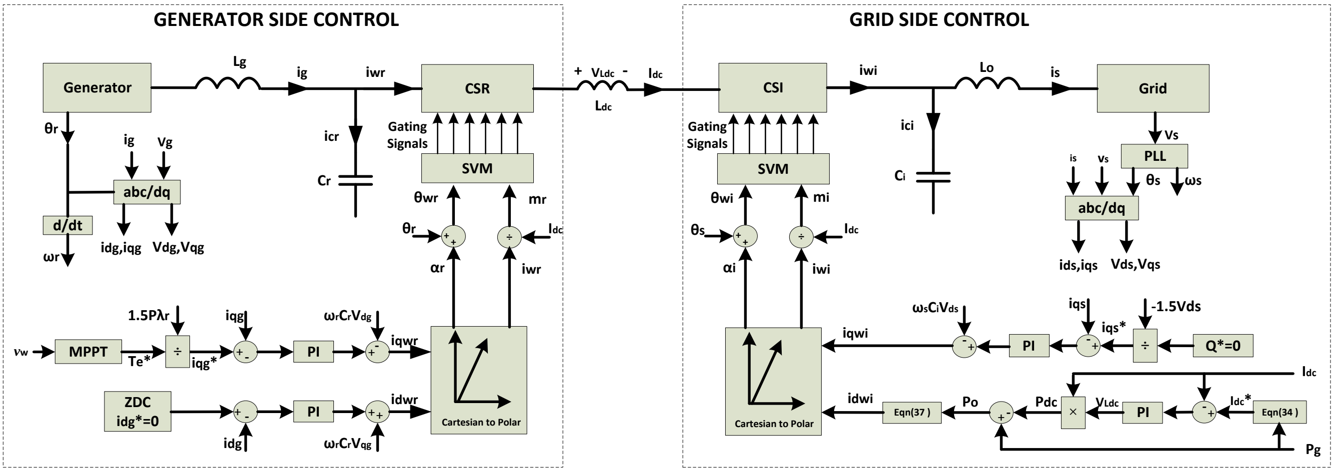

Fig. 3. Control schemes for generator and grid side converters.

Grid is assumed to be stiff and can be simplified as a voltage source with a series inductance L_o, and neglected source resistance.

The CSI output current i_{wi} in d-q axes is given by,

$$i_{dwi} = i_{ds} + i_{dci} \tag{19}$$

$$i_{qwi} = i_{qs} + i_{qci} \tag{20}$$

The CSI output current should supply capacitor and grid currents, the capacitor voltage in d-q axes is given by,

$$(V_{dci} + jV_{qci}) = (V_{ds} + jV_{qs}) - (i_{ds} + ji_{qs})(j\,\omega_s L_o) \tag{21}$$

Hence,

$$V_{dci} = V_{ds} - \omega_s L_o i_{qs} \tag{22}$$

$$V_{qci} = \omega_s L_o i_{ds} \tag{23}$$

Hence the capacitor current in d-q axes is given by,

$$(i_{dci} + ji_{qci}) = (V_{dci} + jV_{qci})(j\,\omega_s C_i) \tag{24}$$

i.e.,

$$i_{dci} = -\omega_s C_i V_{qci} \tag{25}$$

$$i_{qci} = \omega_s C_i V_{dci} \tag{26}$$

By substituting from (22) and (23) into (25) and (26), the expression for capacitor current components can be obtained,

$$i_{dci} = -\omega_s^2 C_i L_o i_{ds} \tag{27}$$

$$i_{qci} = \omega_s C_i V_{ds} - \omega_s^2 C_i L_o i_{qs} \tag{28}$$

For unity power factor operation (Q_o = 0), the quadrature component of the grid current must be equal zero (i_{qs} = 0), thus the CSI d-q axes currents will be,

$$i_{dwi} = (1 - \omega_s^2 C_i L_o) i_{ds} \tag{29}$$

$$i_{qwi} = \omega_s C_i V_{ds} \tag{30}$$

From the foregoing analysis, implementing the reactive power controller is done by comparing the reference zero q-axis grid current with measured one and the error signal is fed to a PI controller as in Fig. 3, and then the CSI q-axis current is simply computed by adding the q-axis capacitor current to the output of the PI controller.

Now the main target is to regulate the dc-link current and controlling the active power flow to the grid, the CSI output current is related to the dc-link current by the modulation index m_i where,

$$m_i I_{dc} = \sqrt{(i_{dwi}^2 + i_{qwi}^2)} \tag{31}$$

Since the dc-link current varies inversely with the modulation index, so in order to get minimum dc-link current thus the switching losses is decreased, the maximum linear modulation index (i.e. m_i = 1) is assumed, also by substituting from (29) and (30) into (31) the dc-link current will be,

$$I_{dc} = \sqrt{(1 - \omega_s^2 C_i L_o)^2 i_{ds}^2 + (\omega_s C_i V_{ds})^2} \tag{32}$$

For same power transfer from generator side to grid side we want,

$$P_g \cong P_o = 1.5 V_{ds} i_{ds} \tag{33}$$

Substituting for i_{ds} in terms of P_g in (32), the reference dc-link current will be obtained as,

$$I_{dc}^* = \sqrt{(1 - \omega_s^2 C_i L_o)^2 \left(\frac{P_g}{1.5\,V_{ds}}\right)^2 + (\omega_s C_i V_{ds})^2} \tag{34}$$

The dc-link current is regulated by comparing its reference by its measured value, and feeding the difference to a PI controller. The PI controller gives the dc-link voltage (V_{Ldc}) which is multiplied by the dc current to give the instantaneous dc-link inductor power.

Since the power difference between generator-side converter and grid-side converter that determines the dc-link inductor power, assuming that the converters are lossless and all the passive components are ideal, we have

$$P_{dc} = P_g - P_o \tag{35}$$

The voltage across the dc link choke is V_{Ldc} and the instantaneous power in the dc link is therefore obtained as,

$$P_{dc} = P_g - P_o = V_{Ldc} I_{dc} = L_{dc} I_{dc} \frac{dI_{dc}}{dt} \tag{36}$$

And at steady state the desired target P_g = P_o will be reached.

By substituting form (33) into (29), The CSI d-axis current component i_{dwi} is given by,

$$i_{dwi} = (1 - \omega_s^2 C_i L_o)\left(\frac{P_o}{1.5 V_{ds}}\right) \quad (37)$$

Where, the value of P_o is deduced form (36), the values of d-q axes currents of the CSI with the dc-link current will fed to the SVM algorithm as previously done in the generator side converter control. Fig. 3 shows the complete control scheme for both converters.

VI. Simulation Results

A simulation model for the system has been built using MATLAB/SIMULINK. The system parameters are listed in Table I. In the simulation, the system is driven by a built in wind turbine model provided by MATLAB/SIMULINK. The turbine model receives the wind speed in (m/s) and the MPPT algorithm provides an optimized reference electromagnetic torque (T_e^*) to the control system.

In order to simulate the transient response of the system controllers, wind speed (v_w) is changed as follows:

Interval I: 8.5 m/s for $0 < t < 1$s,

Interval II: 9.5 m/s for $1\text{s} < t < 2$s,

Interval III: 10.5 m/s for $t > 2$s.

The simulation results are shown in Fig. 4, 5 and 6. The reference torque for MPPT is changed accordingly, as shown in Fig. 4(b). It is obvious that any change in wind speed leads to a corresponding change in the electromagnetic torque and thus the reference current (i_{qg}^*) also changes. Fig. 5(a) shows that the generator current (i_{qg}) has a good performance and it adequately follows its reference at steady state.

With wind speed variation, it is clear that the ZDC controller, the dc-link controller, and the grid reactive power controller follow their references as shown in Fig. 5(b), Fig. 5(c), and Fig. 6(b) respectively.

Fig. 6(a) shows that, as the wind speed changed, the optimum power extracted from the wind will change according to the MPPT algorithm, thus the active power output of the generator is changed, thanks to the dc-link controller and the grid direct current controller the generated power can properly transferred to the grid side.

Finally Fig. 6(b) shows that the reactive power is always zero at any wind speed to achieve a unity power factor operation as targeted.

VII. Conclusion

In this paper, a control scheme for PWM CSC-based PMSG wind energy conversion systems was introduced. The control strategy was developed for independent active and reactive power control while extracting the maximum power from wind. The control system separately decouples the active power and reactive power control through FOC and VOC for the generator side and the grid side respectively. In particular, the dc link current is minimized in steady state to reduce the devices' switching loss and conduction loss for achieving maximum overall efficiency. The introduced control scheme is verified by the simulation on high power rating. Since the introduced system mainly based on PMSG and CSC, it has many advantages such as low maintenance, high efficiency, high power transfer and inherited short circuit protection. These advantages are shown promise for offshore wind energy systems applications.

TABLE I
System Parameters

Generator Parameters	
Rated Mechanical Power	2.45 MW
Rated Mechanical Torque	58.5 kN.m
Rated Speed	400 rpm
Number of Poles	16
Rated Line Voltage	4000 V
Rated Line Current	490 A
Rotor Flux Linkage	9.7462 V.s
Stator d- and q- axes Inductance	9.816 mH
Stator Resistance	24.21 mΩ
Grid Parameters	
Line Voltage	11000 V
Equivalent Inductance	1.3 mH
Frequency	50 Hz
CSC Parameters	
CSI Capacitor	160 µF
CSR Capacitor	120 µF
CSCs Switching Frequency	2 kHz
DC-Link Inductance	0.2 H

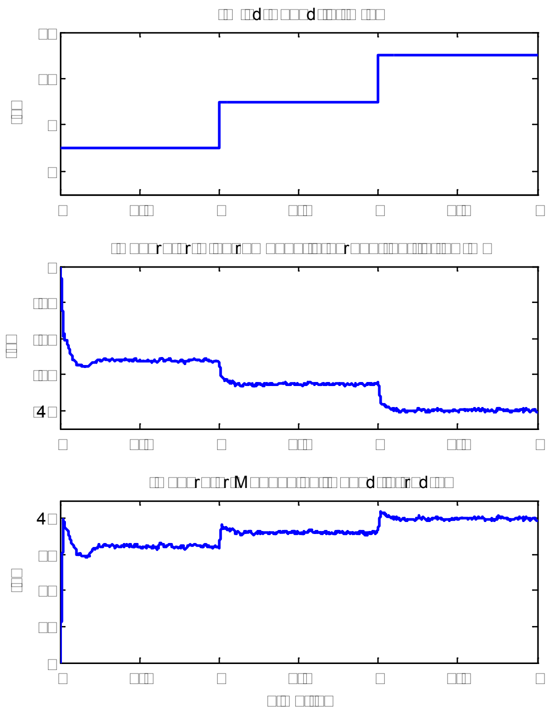

Fig. 4. (a) The wind speed profile. (b) The corresponding electromagnetic torque. (c) The corresponding generator speed.

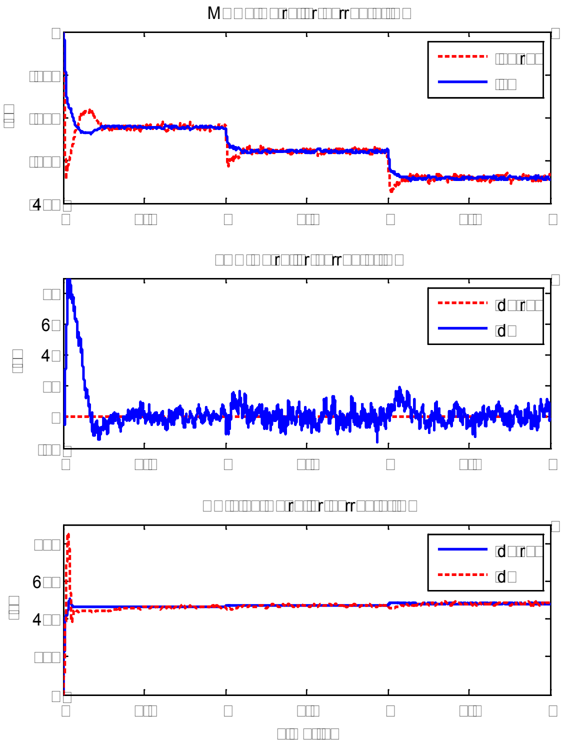

Fig. 5. (a) The MPPT controller response. (b) The ZDC controller response. (c) The DC-Link current controller response.

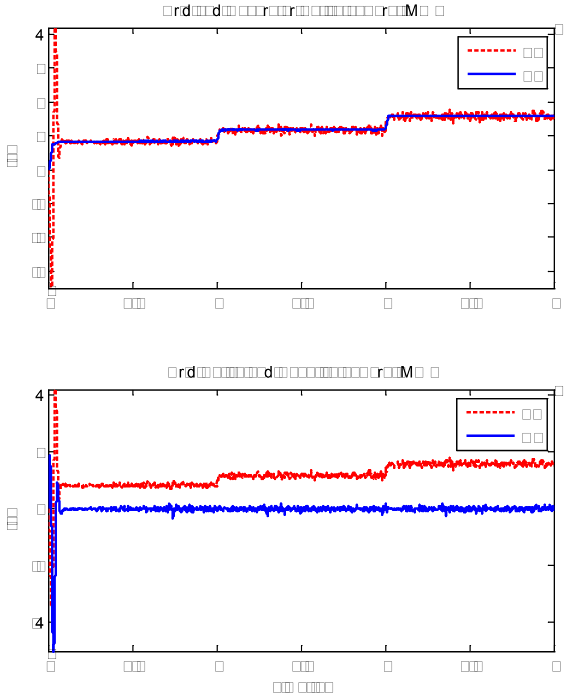

Fig. 6. (a) The grid and generator active powers. (b) The grid active and reactive powers

ACKNOWLEDGMENT

This publication was made possible by NPRP grant NPRP 4-941-2-356 from the Qatar National Research Fund (a member of Qatar Foundation). The statements made herein are solely the responsibility of the authors.

REFERENCES

[1]. Olimpo Anaya-Lara, Nick Jenkins, Janaka Ekanayake, Phill Cartwright, Mike Hughes,Wind Energy Generation Modelling and Control, A John Wiley and Sons, Ltd., Publication 2009.

[2]. Jingya Dai, Dewei (David) Xu, and Bin Wu,"A Novel Control Scheme for Current-Source-Converter-Based PMSG Wind Energy Conversion Systems,"IEEE Trans. Power Electron., vol. 24 , no. 4, pp.963–972, Apr. 2009.

[3]. Jiaqi Liang, Wei Qiao, Ronald Harley,"Feed-Forward Transient Current Control for Low-Voltage Ride-Through Enhancement of DFIG Wind Turbines," IEEE Trans. Energy Convers., vol. 25, no. 3, pp.836–843 , Sep. 2010.

[4]. M. Chinchilla, S. Arnaltes, and J. C. Burgos, "Control of permanentmagnet generators applied to variable-speed wind-energy systems connected to the grid," IEEE Trans. Energy Convers., vol. 21, no. 1, pp.130–135 , Mar. 2006.

[5]. B. Wu, High-Power Converters and AC Drives. New York/Piscataway, NJ: Wiley/IEEE Press, 2006.

[6]. I.A. Gowaid, A. El-Zawawi, M, El-Gammal, " Improved inertia and Frequency Support from Grid- Connected DFIG Wind Farms", IEEE Power Sys. Conference, March 2011.

[7]. Md. Enamul Haque, Michael Negnevitsky, and Kashem M. Muttaqi,"A Novel Control Strategy for a Variable-Speed Wind Turbine With a Permanent-Magnet Synchronous Generator",IEEE Transaction on Industry applications, vol. 46, no. 1, JAN/FEB 2010.

[8]. BinWu, Yongqiang Lang, Navid Zargari, Samir Kouro.,"Power Conversion and Control Of Wind Energy Systems", Wiley-IEEE Press, 2011.

[9]. J. D. Ma, B.Wu, N. R. Zargari, and S. C. Rizzo, "A space vector modulated CSI-based AC drive for multimotor applications ," IEEE Trans. Power Electron., vol. 16, no. 4, pp. 535–544, Jul. 2001.

[10]. B.Wu, J. Pontt, J. Rodriguez, S. Bernet, and S.Kouro, " Current-source converter and cycloconverter topologies for industrial medium-voltage drives," IEEE Trans. Ind. Electron., vol. 55, no. 7, pp. 2786–2797, Jul. 2008.

[11]. L. Benchaita, S. Saadate, and A. Salem nia, "A comparison of voltage source and current source shut active filter by simulation and experimentation," IEEE Trans. Power Syst., vol. 14, no. 2, pp. 642–647, May 1999.

[12]. Jingya Dai, Dewei (David) Xu, BinWu,and Navid R. Zargari,"Unified DC-Link Current Control for Low-Voltage Ride-Through in Current-Source-Converter-Based Wind Energy Conversion Systems,"IEEE Trans. Power Electron., vol. 26, no. 1, pp. 288–297, Jan. 2011.

[13]. Jingya Dai, Dewei Xu, Bin Wu, Navid R. Zargari, Yongqiang Lang,"Dynamic Performance Analysis and Improvements of a Current Source Converter Based PMSM Wind Energy System,"IEEE, PESC 2008.